Option Pricing Using Local Volatility Function:
How to Specify its Knots?

Mr. Wisuth Raweerojthanatt

การคำนวณราคาออปชั่นด้วยการระบุจุดปมของฟังก์ชั่นความผันผวนแบบโลคอล

นายวิสุทธิ์ รวีโรจน์ธนัท

Independent Study Title	Option Pricing Using Local Volatility Function: How to Specify its Knots?
By	Mr. Wisuth Raweerojthanatt
Field of Study	Financial Engineering
Thesis Advisor	Associate Professor SIRA SUCHINTABANDID, Ph.D.

Accepted by the FACULTY OF COMMERCE AND ACCOUNTANCY, Chulalongkorn University in Partial Fulfillment of the Requirement for the Master of Science

INDEPENDENT STUDY COMMITTEE

.... Chairman
(Associate Professor THAISIRI WATEWAI, Ph.D.)

.... Advisor
(Associate Professor SIRA SUCHINTABANDID, Ph.D.)

.... Examiner
(TANAWIT SAE SUE, Ph.D.)

จุฬาลงกรณ์มหาวิทยาลัย
CHULALONGKORN UNIVERSITY

วิสุทธิ์ รวีโรจน์ธนัท : การคำนวณราคาออปชั่นด้วยการระบุจุดปมของฟังก์ชั่นความผันผวนแบบโลคอล. (
Option Pricing Using Local Volatility Function: How to Specify its
Knots?) อ.ที่ปรึกษาหลัก : รศ. ดร.สิระ สุจินตะบัณฑิต

พิจารณาโมเดลฟังก์ชั่นการแพร่กระจายหนึ่งตัวแปรต่อเนื่อง ร่วมกับสมการรูปแบบทั่วไปของแบล็คสโคลส์ เพื่อ
ประเมินราคาออปชั่นแบบยุโรปของสินทรัพย์ใดๆ กำหนดจำนวนของจุดปมความผันผวน และตำแหน่งบนระนาบของราคาหุ้น
และเวลาหมดอายุในหลายๆรูปแบบ พิจารณาจุดปมความผันผวนเสมือนว่าเป็นตัวแปรการตัดสินใจ ใช้ฟังก์ชั่นเส้นโค้งแบบไบ
คิวบิกในการประมาณค่าฟังก์ชั่นความผันผวนแบบโลคอลด้วยจุดปมดังกล่าว และทำการหาค่าที่เหมาะสมที่สุดของจุดปมความ
ผันผวนแบบไม่เป็นเส้นตรงและมีเงื่อนไข โดยเทียบค่าของออปชั่นที่ได้จากการคำนวณกับข้อมูลได้ที่จากตลาด ใช้ข้อมูลดัชนี
SET50 เป็นข้อมูลจากตลาดเพื่อทดสอบความแม่นยำในการประเมินราคาด้วยการกำหนดจุดปมรูปแบบต่างๆ และทำการ
ทดสอบโดยการใช้ค่าความผันผวนที่ได้จากการปรับเทียบด้วยกลุ่มข้อมูลหนึ่ง ไปประเมินราคาออปชั่นในวันถัดออกไปที่อยู่
นอกเหนือกลุ่มข้อมูลที่ใช้ปรับเทียบจุดปม แสดงรูปแบบของพื้นผิวของฟังก์ชั่นความผันผวนที่ประเมินราคาได้แม่นยำใกล้เคียง
กับตลาด

| สาขาวิชา	วิศวกรรมการเงิน	ลายมือชื่อนิสิต ....
ปีการศึกษา	2563	ลายมือชื่อ อ.ที่ปรึกษาหลัก ....

6182954026 : MAJOR FINANCIAL ENGINEERING
KEYWOR
D:
Optimization, Local Volatility Function, Volatility Knot, Volatility Surface, Generalized Black-Scholes Equation, SET50 Index, European Option, Option Pricing

Wisuth Raweerojthanatt : Option Pricing Using Local Volatility Function: How to Specify its Knots?. Advisor: Assoc. Prof. SIRA SUCHINTABANDID, Ph.D.

European options of an asset are priced following a continuous 1-factor diffusion model and the generalized Black-Scholes equation. Volatility knots are determined by many specifications that are the number and the location of knots at any stock price and time to expiration. Considering the volatility knots as a set of decision variables, we can approximate the local volatility function with a bicubic spline function to compute option values fitted to a finite set of market data by solving a constrained nonlinear optimization problem. With the real market data of SET50 Index options, pricing accuracy of different knots' specifications are demonstrated. The experiment in using a set of volatility knots to price options that are out of the calibrated dataset is also provided. The patterns of volatility surface that approximates option values sufficiently close to the market are illustrated.

จุฬาลงกรณ์มหาวิทยาลัย
CHULALONGKORN UNIVERSITY
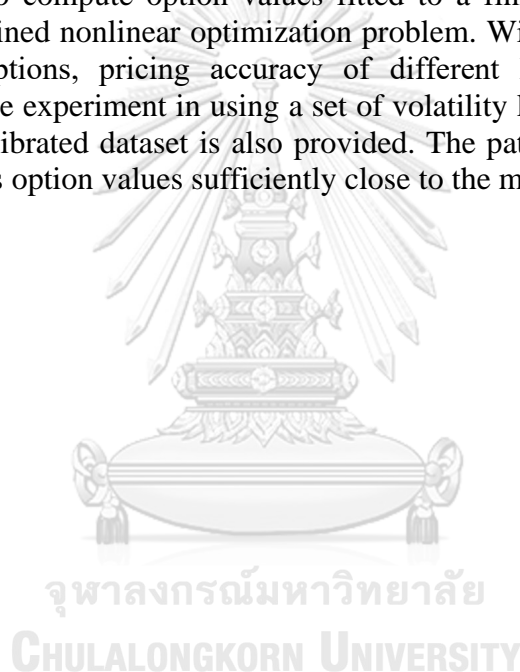
Field of Study:	Financial Engineering	Student's Signature ....
Academic Year:	2020	Advisor's Signature ....

ACKNOWLEDGEMENTS

TABLE OF CONTENTS

Page

LIST OF TABLES

LIST OF FIGURES

Page

1. Introduction.

European options are usually estimated by some numerical models [4, 14, 18, 19] that have been introduced and developed to obtain the most reasonable price. Various models probably perform differently but generally compute from the underlying price of those options and other market variables, e.g. the volatility [4, 19].

The constant-volatility Black-Scholes model [4, 19] is widely used in financial practice because its complexity level is not as high as others. Its simplicity is only to assume one constant volatility for all the options of a related security; nevertheless, recent evidence shows that only using one constant volatility is insufficient [20, 21]. According to any underlying, several put and call options that have different strike prices and expiration dates are traded on a single day; as a result, one value of the volatility cannot possibly match all the options. Pragmatically, the constant-volatility Black-Scholes model is relaxed and applied by considering different volatility values referring to different strikes and maturities [7, 14, 18]. These volatility values will be mentioned as *market implied volatility*, or MIV in short, later on in this paper. Even though this idea seems fine for pricing each European option individually, the options with the same underlying should, in principle, have the same volatility function following the 1-factor continuous diffusion approach,

$$dS_t/S_t = \mu(S_t, t)dt + \sigma^*(S_t, t)dW_t, \quad t \in [0, \tau], \quad \tau > 0. \tag{1}$$

To describe the variables, W_t is a standard Brownian motion, and τ is a fixed trading horizon. We define that the asset value at any time t is S_t and assume its initial value S_{int}. The functions of return rate $\mu(S_t, t)$ and *local volatility* $\sigma^*(S_t, t)$ are deterministic real numbers that depend on stock price S_t at time t. It is obvious that computing the volatility values individually for different strikes and maturities violates the equation (1); in other words, this idea sometimes evokes diverse values of volatility for a pair of stock price and time and confuses modelers in what the volatility really is.

Some approaches [7, 12, 14, 18] have been developed from (1) and proposed to construct another type of the local volatility function, called the *volatility surface* $\sigma(s, t)$ by mainly considering the asymmetry of the volatility in the possible range of asset price s and time to expiration t. On the other hand, since $\sigma(s, t)$ cannot

be observed directly from the market like the constant-volatility case, there is an idea to imply the volatility surface from the market option price data [1, 12]. By considering under the no arbitrage assumption of the observable European option prices at all strikes and maturities [19], the local volatility function can be uniquely determined with many ways of calibration methods [1, 12]. As far as I have acknowledged, the specific shape of the volatility surface is still ambiguous [6]. However, the volatility function is possibly nonlinear and unable to solve without an approximation, so a discretization method is required [1, 2, 16]. We, thus, discretize stock prices s and time to expiration t into small *grids* that fit all the possible range of the volatility surface $\sigma(s,t)$.

Ideally, we can obtain the most accurate result of the surface by using very fine grids for both s and t; in this case, we have to create infinite discretization points. A computational issue, therefore, occurs while solving this optimization problem because the number of implied volatility values is large [1, 2, 5, 9, 10, 12, 15, 16, 20]. This means that we solve a big number of decision variable problem with limited market data, so the result cannot be computed easily. To manage this difficulty, we need to set a smaller number of discretization points in both s and t and allow some tolerated error. To do this, a limited number of *knots* is introduced to represent the whole volatility surface [5, 9, 15, 20]. Since fewer discretized points for a nonlinear function solving lead to a coarser result, one of the most typical approaches is to use a bicubic spline *function* [24] that is one of regularization methods [22-24] to perform smoothness of a considered function in an approximation problem. At a small number of knots, approximation results with a *bicubic spline function* [3, 10], considering in two dimensions, can cover the whole boundary of s and t. Nonetheless, the number and location of knots is likely to cause different results in both pricing accuracy and computational time [11, 24].

Besides, when a financial institute generates a volatility surface in practice, it is used to price option values for some period. One of the questions in mind is that how long we can keep using the fitted volatility surface without recalibration. If the previously generated volatility surface does not match with the current market, it will create a mispricing problem. Although an institute can theoretically calibrate the

volatility surface every time for the best accuracy in pricing, the cost in computational time also matters.

In this report, we propose a bicubic spline functional approach for smoothing the volatility surface from some representative knots that are chosen at different numbers and locations. The knot's number is considered from the minimum number that a bicubic spline function can generate a non-flat surface; on the contrary, the number of knots should not be greater than the number of option market prices to avoid an underdetermined problem. An optimization problem is possibly underdetermined when the number of decision variables is greater than the dimension of objective function. Later, we locate the knots in different positions within the boundary of possibly stock price and time to expiration. Given initial volatility values at all knots, the implied volatility knots are acquired by solving a *constrained nonlinear optimization problem* with a bicubic spline function to match as close as possible the market option. After that, we analyze the effects of each knot specification in term of accuracy and also provide a method to observe the ability to keep using a fitted volatility surface for an extend period of time before having to recalibrate. Finally, we end up with a tendency of volatility surface's pattern from all the results in the previous parts.

This paper starts with the research questions and objectives in Section 2. All the following methodologies are explained in Section 3. The steps in acquiring the examples of numerical data, SET50 Index options and other related variables, are shown in Section 4. After applying all the methodologies with the real data, the experimental results can be shown in Section 5, and the conclusion of this work is finally stated in Section 6.

2. Research Questions and Objectives.

2.1. What is the appropriate number of the implied volatility surface's knots for pricing European options in Thailand with a bicubic spline technique?

To solve an optimization problem with the same objective function, a large number of decision variables tends to generate better results than a smaller number; in contrast, more decision variables imply longer time in computation. Furthermore, a bicubic spline function of one variable requires at least three coordinates to create a curvature. However, the local volatility function depends on two variables, stock price s and time to expiration t, so we need at least four coordinates of (s, t) to create a non-flat surface. Regarding to a theory of *volatility smile* [7, 14, 18], when we plot implied volatility values with respect to different strike prices, the shape of the result looks like a smile. To draw a curve of smile, we need at least three considered points: one is at the lowest position of smile, and the other two points are located on the left and right of the first one but higher. Since a stock price shares the same currency unit with a strike price, it is possible that the shape of volatility values with respect to stock prices is also a smile. When we combine both the mathematical limitation and the possible effect of the volatility smile together, we test the results with different numbers of knots from the possible minimum number which is 4 to the maximum number that still matters. We hypothesize that five knots should be appropriate to generate volatility surfaces for pricing options and back this up with numerical result in Sub-section 5.1.

2.2. What are the appropriate locations in placing the implied volatility surface's knots for pricing European options in Thailand?

Other than having many possibilities of knots' number in Sub-section 2.1, those knots can be located anywhere in their boundary space. The idea to specify the knots' location is further shown and explained in Sub-section 3.2, Figure 2. In brief, we should locate the volatility knots at around the initial stock price on s axis and small values of t. Nevertheless, we also apply the concept in Sub-section 2.1: on a given day, the characteristics of market data, e.g., the shape of the implied volatility curve, possibly determine the location of knots to price options accurately. Speaking

of the benefit of this study, if we specify the initial location of knots appropriately, we will possibly not only maintain the acceptable accuracy but also reduce the time in computation of the searching algorithm. To explain about the experiment of this sub-section concisely, we place a group of five volatility knots at several possible locations and find some common properties of the suitable locations. We believe that placing all the knots near the initial stock price S_{int} and the current time or $t = 0$ can generate an appropriate volatility surface in pricing options. However, we will test our belief with empirical data in Sub-section 5.2.

2.3. How long can we keep using the fitted volatility surface without having to re-estimate for pricing European options in Thailand?

As far as we have acknowledged, volatility does not have a stationary property [13], so using a volatility surface for an extended period of time without re-estimation may cause a mispricing problem. However, the volatility function in (1) assuming current option prices can look-forward into future volatility values, so we probably price options in the future with the volatility surface at the present. Anyhow, this paper provides an idea to validate different specifications of the volatility knots that can price options for an extended period of time without recalibration in Sub-section 5.2. This study shows a tendency of appropriate time for recalibrating the volatility surface acquired by reasonable specifications from Sub-section 2.1 and 2.2 to reduce a possibility of mispricing occurrence. If a specification of volatility knots is good, we should be able to keep using it for a week before recalibration. Some concrete evidence will be provided in Sub-section 5.3.

2.4. Does the volatility surface for pricing European options in Thailand have any specific pattern of shape?

Although we have the results from the prior research questions, different values, numbers, and locations of volatility knots may generate various patterns of volatility surfaces. Some of them can be used to price options sufficiently close to the market and might have some common pattern. If we can foresee a pattern of volatility

surfaces, we will possibly set the initial values of the volatility knots more precisely than having no information. As a result, the searching algorithm of the calibration process technically work more quickly. To guess a pattern of volatility surfaces, since strike prices share the same unit with their underlying prices, the cross-section of volatility surface taken perpendicular to t-axis possibly has some curvy pattern, such as a smile shape, as similar as the MIV plot with respect to strike prices. Furthermore, by fixing the price of an underlying at any constant, its call option prices generally decrease with respect to the increment of strikes, but the put option prices go opposite. To hold the 1-factor continuous diffusion approach, however, we should be able to use a volatility surface to price both put and call options at the same time, and we may consider $s = S_{\text{int}}$, which implies strike at the money, as the plane that separates two parts of the volatility surface symmetrically. On the contrary, the real market does not have many options with different time to maturity, so the MIV plot with respect to time to maturity does not have varied shapes comparing to the plot with strikes. We often see the MIV plot with respect to time to maturity forms either an increasing or decreasing line. In our view, the cross-section of the volatility surface taken perpendicular to s-axis is possibly more linear than the cross-section taken perpendicular to t-axis, but the more nonlinearity of the plot with respect to t should fit the market better. To gather all the hypotheses altogether, by cross-sectioning the volatility surface that sufficiently fits the market perpendicular to t-axis, we expect to see a smile, and the vertex of that curve should be located at around $s = S_{\text{int}}$. On the other hand, the cross-section of that surface taken perpendicular to s-axis should form a curve that is not very nonlinear.

3. Methodologies.

3.1. Overview.

To respond to all the research questions, we start with an assumption that at any time t, an underlying price S_t follows a continuous 1-factor diffusion process with the initial value S_{int},

$$dS_t/S_t = \mu(S_t, t)dt + \sigma^*(S_t, t)dW_t, \quad t \in [0, \tau], \quad \tau > 0,$$

where W_t is a standard Brownian motion, and τ is a fixed trading horizon. The deterministic functions of return $\mu(s,t)$ and volatility $\sigma^*(s,t)$ are $\mathcal{R}^+ \times [0,\tau] \to \mathcal{R}$ and sufficiently well behaved to guarantee that (1) has a unique solution [17]. In this paper, we assume that the instantaneous interest rate r and the dividend rate q are constant and greater than zero for simplicity.

Under the no arbitrage assumption [19], the volatility function is applied for all strikes and maturities. Let K be a strike price and T be the time to maturity of an option. There exists a volatility function $\sigma(s,t)$ of an underlying price s at time to expiration t, such that the call price $v_C(\sigma(s,t),K,T)$ and put price $v_P(\sigma(s,t),K,T)$ are unique [2, 5, 9, 10, 12, 15, 16, 20]. Since this paper considers both call and put options with the condition that the volatility at the same s and t values is maintained, the values of both call and put option can be simply represented in a vector format,

$$v(\sigma(s,t),K,T) = \begin{bmatrix} v_C(\sigma(s,t),K,T) \\ v_P(\sigma(s,t),K,T) \end{bmatrix}.$$

Assume that an asset has totally N_M market options corresponding to the strike prices and maturities $\{(K_n,T_n)\}_{n=1}^{N_M}$, the option values with different strikes K_n and maturities T_n can be represented by

$$v_n\big(\sigma(s,t)\big) \overset{\text{def}}{=} v(\sigma(s,t),K_n,T_n), \quad n = 1, \ldots, N_M.$$

Using the market information, we can approximate the values of call and put options. We consider the values approximation as a nonlinear optimization problem to minimize the difference between the market and the model prices by locating the volatility knots $\sigma(s,t)$, which are the decision variables, with some approximation method. Since there are many steps to acquire the required volatility function and its following results, we present Figure 1 to demonstrate the overall process of this paper. At the beginning, we need to specify initial volatility knots and use a smoothing technique that is a bicubic spline function for this paper to create a volatility surface. The surface is used to approximate the model option values that are calibrated with the market prices to acquire the fitted volatility knots. Later, we choose different numbers and locations of the volatility knots to analyze the effect in computing option prices while the characteristics of market data, such as the daily MIV curve, are also

considered. Moreover, we try to see that how long a volatility surface can price options without recalibration. Finally, the results from the preceding analyses possibly show some patterns of the fitted volatility surfaces.

```
┌─────────────────────────────────────────────────────┐
│   Assign Initial Volatility Knots and Create the Surface │
└─────────────────────────────────────────────────────┘
                         ↓
┌─────────────────────────────────────────────────────┐
│            Compute the Model Option Prices           │
└─────────────────────────────────────────────────────┘
                         ↓
┌─────────────────────────────────────────────────────┐
│    Calibrate the Volatility Knots with Market Option Prices │
└─────────────────────────────────────────────────────┘
                         ↓
┌─────────────────────────────────────────────────────┐
│         Analyze Different Specifications of Knot     │
└─────────────────────────────────────────────────────┘
```
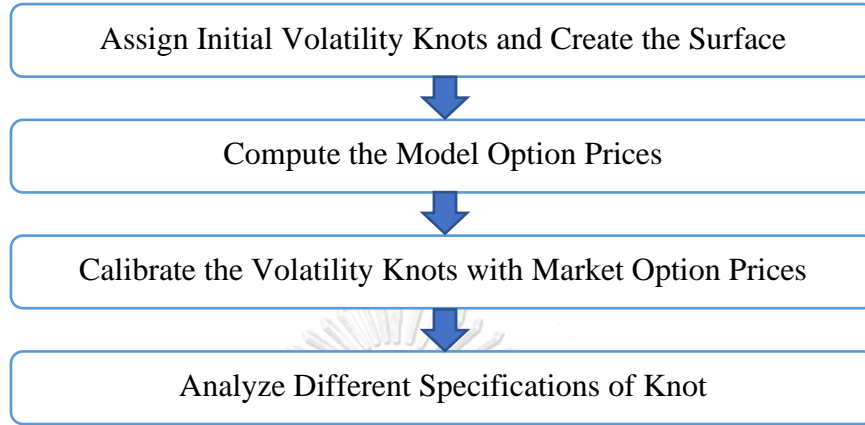
Figure 1*: Overall Process*

3.2. Initial Volatility Surface Set by Bicubic Spline Function.

According to Sub-section 3.1, we need to use some approximation technique [1, 2, 16] to locate the volatility knots and price the options. To start with, we discretize both the stock price s and time to expiration t into grids to ensure that the volatility surface $\sigma(s, t)$ can cover all the possibility ranges of s and t. Let $\mathcal{S}$ and $\mathcal{T}$ be the possible measurable space of s and t accordingly.

$$\mathcal{S} = \{s_i\}, \quad i = 1, \dots, N_s, \quad s_i > s_{i-1}, \quad \text{and}$$
$$\mathcal{T} = \{t_j\}, \quad j = 1, \dots, N_t, \quad t_j > t_{j-1}. \tag{2}$$

To make the applicable $\mathcal{S}$ and $\mathcal{T}$ for all the considered options, s_i and t_j must be in specific ranges that can be defined as following, for $\beta_s \geq 0$ and $\beta_t \geq 0$,

$$\alpha_s = \beta_s K_{\text{all}} + (1 - \beta_s) S_{\text{int, all}},$$
$$s_1 = \max\{\min(\alpha_s), 0\},$$
$$s_{N_s} = \max(\alpha_s),$$
$$t_1 = 0, \qquad\qquad \text{and}$$
$$t_{N_t} = \beta_t \max(T_{\text{all}}),$$

where the subscription "all" refers to all collected data; for instance, K_{all} implies a vector of all strike prices we have, or $K_{\text{all}} = [K_1 \quad \cdots \quad K_{N_M}]$. β_s is a specific real number greater than zero to assure that all the cases of very deep-in-and-out-the-money option are considered, and β_t is another constant multiplier to extend the boundary of the time to expiration axis.

Next, to create a volatility surface with a bicubic spline function, we assume the volatility knots that can represent the whole surface and let p be the number of knots that should be greater than three to create a non-flat surface but no more than the number of market options N_M to avoid an underdetermined problem, or $3 < p \leq N_M$. In this paper, we want to analyze the number of knots that depends on both stock price and time to expiration. For $k = 1, \ldots, p$, we can write $(\hat{s}_k, \hat{t}_k)$ to specify the kth knot coordinate on $\mathcal{S} \times \mathcal{T}$ corresponding with its volatility value $\hat{\sigma}_k \overset{\text{def}}{=} \sigma(\hat{s}_k, \hat{t}_k)$. Furthermore, we can represent all knots in a vector format by

$$
\begin{aligned}
\hat{s} &= [\hat{s}_1 \quad \cdots \quad \hat{s}_p]', \quad s_1 \leq \hat{s}_k \leq s_{N_s}, \\
\hat{t} &= [\hat{t}_1 \quad \cdots \quad \hat{t}_p]', \quad t_1 \leq \hat{t}_k \leq t_{N_t}, \quad \text{and} \\
\hat{\sigma} &= [\hat{\sigma}_1 \quad \cdots \quad \hat{\sigma}_p]'.
\end{aligned}
\tag{3}
$$

After that, to create a cubic spline function replicating $z(x, y)$ for any values x and y, some representatives of x, y and $z(x, y)$ are required. We may let $\hat{x}$ and $\hat{y}$ be vectors at the same size to be some representatives of x and y respectively, so $\hat{z} \overset{\text{def}}{=} z(\hat{x}, \hat{y})$ is a vector representing some values of $z(x, y)$. For a notating purpose in this paper, the bicubic spline function can be written by $z(x, y) \overset{\text{def}}{=} \text{BCS}(x, y; \hat{z})$. It is computed by combining two Matlab functions: the detail why we use this combination to approximate the bicubic spline function is explained in Sub-section 3.6. Hence, we can obtain a volatility surface by taking the volatility knots $\hat{\sigma}$ with all the considered values of s_i and t_j in (2) into the bicubic spline function that

$$
\sigma_{i,j} = \sigma(s_i, t_j) \overset{\text{def}}{=} \text{BCS}(s_i, t_j; \hat{\sigma}).
$$

3.3. Model Option Price Computation.

There are several approaches to obtain the option values. In this paper, we use the idea of the generalized Black-Scholes equation [19],

$$\frac{\partial v}{\partial t} + (r - q)s\frac{\partial v}{\partial s} + \frac{1}{2}\sigma^2 s^2 \frac{\partial^2 v}{\partial s^2} = rv, \tag{4}$$

where v refers to the option price, the risk-free interest rate r and the dividend rate q are constants acquired from the market information, and σ implies the volatility function $\sigma(s,t)$ at any stock price s and time to expiration t. With the boundary conditions,

$$v_C(\sigma(s,T),K,T) = \max(s - K, 0),$$
$$v_P(\sigma(s,T),K,T) = \max(K - s, 0),$$
$$\lim_{s\to\infty}\frac{\partial}{\partial s}v_C(\sigma(s,t),K,T) = \frac{\partial}{\partial s}v_P(\sigma(0,t),K,T) = e^{-q(T-t)}, \quad t \in [0,T], \quad \text{and}$$
$$\lim_{s\to\infty}v_P(\sigma(s,t),K,T) = v_C(\sigma(0,t),K,T) = 0, \quad\quad t \in [0,T].$$

Since European options of a security typically have various maturity times $\{T_n\}_{n=1}^{N_M}$, it is possible to have some time to expiration $t_j > T_n$. This is commonly known as an expired option: an option that is held after the maturity date has no price. In other words, we can neglect the option price $v(\sigma(s,t),K,T)$ at any $t > T$. Meanwhile, by realizing the third and last boundary conditions of (4), when s_1 and s_{N_s} are set appropriately, we can imply that

$$\frac{\partial}{\partial s}v_C(\sigma(s_{N_s},t),K,T) = \frac{\partial}{\partial s}v_P(\sigma(s_1,t),K,T) \approx e^{-q(T-t)}, \quad t \in [0,T], \quad \text{and}$$
$$v_P(\sigma(s_{N_s},t),K,T) = v_C(\sigma(s_1,t),K,T) \quad \approx 0, \quad\quad t \in [0,T].$$

Consequently, at any $n = 1, \dots, N_M$ of the nth option with the volatility surface from Sub-section 3.2, the option values at which coordinates (s_1,t), (s_{N_s},t) and (s,T_n) for any values of s and t in $\mathcal{S} \times \mathcal{T}$ are initially defined, and the remaining values on other coordinates (s_i,t_j) can be approximated by the explicit finite difference method. Thus, we have the model option prices $v_n(\sigma(s,t))$ for all $n = 1, \dots, N_M$.

3.4. Calibration of Volatility Knots.

As we assume that an asset has N_M market options, the option bid-ask pairs can be written as

$$\{(\text{bid}_n, \text{ask}_n)\}_{n=1}^{N_M} = \begin{bmatrix} \{(\text{bid}_{C,n}, \text{ask}_{C,n})\}_{n=1}^{N_M} \\ \{(\text{bid}_{P,n}, \text{ask}_{P,n})\}_{n=1}^{N_M} \end{bmatrix}$$

The subscription C and P refer to the option's types which are call and put sequentially. However, the option values are expected to be as close as possible to the market data, so a boundary condition can be set by

$$\text{bid}_n \leq v_n(\sigma(s,t)) \leq \text{ask}_n, \quad n = 1, \ldots, N_M, \tag{5}$$

assuming that the underlying has price s at time t. After that, the option values $\{v_n(\sigma(s,t))\}_{n=1}^{N_M}$ can be considered as an *inverse function approximation problem* of $\{(\text{bid}_n, \text{ask}_n, K_n, T_n)\}_{n=1}^{N_M}$ that is finite and observable from the market. The volatility values for any stock price and time to expiration are expected to be the result of this problem. Let Σ denote the space of measurable functions in the region $[0, \infty) \times [0, \tau]$. Referring to Sub-section 3.2, we can consider that a volatility function is approximated from a bicubic spline technique, $\sigma(s,t) \overset{\text{def}}{=} \text{BCS}(s,t; \hat{\sigma})$; therefore, we can define an optimization problem,

$$\min_{\hat{\sigma} \in \Sigma} \sum_{n=1}^{N_M} \left[\{\text{bid}_n - v_n(\text{BCS}(s,t; \hat{\sigma}))\}^+ + \{v_n(\text{BCS}(s,t; \hat{\sigma})) - \text{ask}_n\}^+ \right], \tag{6}$$

where $x^+ \overset{\text{def}}{=} \max(x, 0)$. Alternatively, the mid-price, $\text{mid}_n \overset{\text{def}}{=} (\text{bid}_n + \text{ask}_n)/2$, is obviously more beneficial to solve for the option values by a variational least squares problem,

$$\min_{\hat{\sigma} \in \Sigma} \sum_{n=1}^{N_M} \left[v_n(\text{BCS}(s,t; \hat{\sigma})) - \text{mid}_n \right]^2, \tag{7}$$

than solving (5) directly. It is distinct that one pair of $v(\sigma(s,t), K, T)$ values can be obtained by infinite number of $\hat{\sigma}$ solutions. For any strike K and maturity T, there exists a volatility function $\sigma(s,t)$, such that the generated option value, $v_C(\sigma(s,t), K, T)$ or $v_P(\sigma(s,t), K, T)$, acceptably fit the market data, either the bid-ask

pair or mid-price. In conclusion, the implied volatility function $\sigma(s,t)$ is acquired by solving one of $(5,6,7)$ with the limited observable data in the market.

For practical purpose, all the elements in $\hat{\sigma}$ can be bounded in some region, and each knot possibly affects the computation of option values differently. To manage these conditions, let l and u denote the vectors that contain lower and upper bounds of the volatility knots, respectively. We can write a constrained optimization problem,

$$\min_{\hat{\sigma} \in \Sigma} f(\hat{\sigma}) = \sqrt{\sum_{n=1}^{N_M} \left[w_n \{ v_n \big(\mathrm{BCS}(s,t;\hat{\sigma}) \big) - \mathrm{mid}_n \} \right]^2}, \tag{8}$$

$$\text{subject to} \quad l \leq \hat{\sigma} \leq u,$$

where w_n is the weight of the nth considered option in computation. The application of w_n in (8) can be helpful when we want to weight differently according to each option's necessity. However, this paper considers the equally-weighted case, $w_1 = \cdots = w_{N_M} = 1/N_M$, to fix the equal importance to all considered options because we want to study the effect of knot specification that can apply to all options traded in the market.

3.5. Specification of Knots.

This paper studies the effects of knots in different specifications, but the boundary conditions in (3) are still held to maintain the possible measurable space of $\mathcal{S}$ and $\mathcal{T}$ in (2). However, to define the knots more specifically, we can write that for any $\gamma_{s,k} \in \mathbb{R}$ and $\gamma_{t,k} \in [0,\infty)$,

$$\begin{aligned}
\delta_{s,k}^- &= \min\{ (1 + \gamma_{s,k})S_{\text{int, cal}} - \gamma_{s,k}K_{\text{cal}} \}, \\
\delta_{s,k}^+ &= \max\{ \gamma_{s,k}K_{\text{cal}} + (1 - \gamma_{s,k})S_{\text{int, cal}} \}, \\
\hat{s}_k &= \begin{cases} \max(\delta_{s,k}^-, s_1), & \gamma_{s,k} \leq 0 \\ \min(\delta_{s,k}^+, s_{N_s}), & \gamma_{s,k} > 0 \end{cases} \quad \text{and} \\
\hat{t}_k &= \min(\gamma_{t,k}\max(T_{\text{cal}}), t_{N_T}),
\end{aligned} \tag{9}$$

where the subscription "cal" implies a considered set of observable data for calibrating knots. Indeed, $\gamma_{s,k}$ is a multiplier to adjust $\hat{s}_k$ to move away from $s = S_{\text{int}}$; meanwhile, when $\gamma_{t,k}$ increases, $\hat{t}_k$ moves away from zero to t_{N_T}. To describe more specifically, $\hat{s}_k$ is at S_{int} when the value of $\gamma_{s,k}$ is zero. For negative $\gamma_{s,k}$, it gives a direction of knot's movement from $s = S_{\text{int}}$ to $s = s_1$; on the contrary, positive $\gamma_{s,k}$ moves $\hat{s}_k$ to another direction or $s = s_{N_s}$. To summarize the knotted adjusting values, we may consider that

$$\Gamma = \begin{bmatrix} \gamma_{s,1} & \gamma_{t,1} \\ \vdots & \vdots \\ \gamma_{s,p} & \gamma_{t,p} \end{bmatrix};$$

nonetheless, there are many number of p in specifying Γ, so we may define Γ_p as a knotted adjusting matrix Γ with p knots. In addition, within the same number of knots, it is possible that the knotted adjusting values can be chosen differently; thus, we determine $\Gamma_{p,\hat{p}}$ as the $\hat{p}^{\text{th}}$ specification of Γ_p. Since a vector $\hat{\sigma}$ relate to the values of $\hat{s}_k$ and $\hat{t}_k$ for $k = 1, \dots, p$, we can consider $\hat{\sigma}_{p,\hat{p}}$ as a set of volatility knots from specifying $\Gamma_{p,\hat{p}}$ or Spec. p-$\hat{p}$.

Regarding to Sub-section 3.1, the generated option value is a function of K, T, s, t and $\sigma(s,t)$ variables, and it is obvious that K and T relate to s and t accordingly. To search the best set of knots' coordinates at any (s,t), we may firstly consider candidates of $\hat{s}_k$ that are possibly in between the maximum and minimum of observable strike prices. Moreover, since $\sigma(s,t)$ term does not exist in computation of the third and fourth boundary conditions in (4), this implies that the option values at very deep-in-and-out-the-money are considered less volatile than the values at the money; otherwise, specifying $\hat{s}_k$ at around $s = S_{\text{int}}$ is possibly better than other prices that are further away. $\hat{t}_k$'s candidates, on the other hand, should not be greater than the maximum of observable time to maturity. Additionally, observable options have different values of maturity time T_m where $m = 1, \dots, N_T$ and $T_1 < \cdots < T_{N_T}$, and (4) is solved by approximating the option values from $t = T_m$ to $t = 0$ for each option individually. The computational process clearly occurs more frequently at a smaller number m of $t = T_m$ than the greater one; as a result, specifying smaller values of $\hat{t}_k$

is probably more appropriate. Since adjusting values of $\gamma_{s,k}$ and $\gamma_{t,k}$ directly relate to $\hat{s}_k$ and $\hat{t}_k$ on s-t plane, we can summarize possible locations of a knot by observing Figure 2: the dark areas are more likely to have knots than the light ones. Our main goal, however, is to select some coordinates $(\hat{s}_k, \hat{t}_k)$ for $k = 1, \dots, p$ of knots to generate a volatility surface that can approximate option values as close as the market prices. In other words, the knots' specification that we choose has to create a small value of the objective function in (8), and more details are shown in Section 5.

$\gamma_{(s \text{ or } t),k}$	$\hat{s}_k$	$\hat{t}_k$
-1	$\min(K_{\text{cons}})$	$-$
0	S_{int}	0
1	$\max(K_{\text{cons}})$	$\max(T_{\text{cons}})$
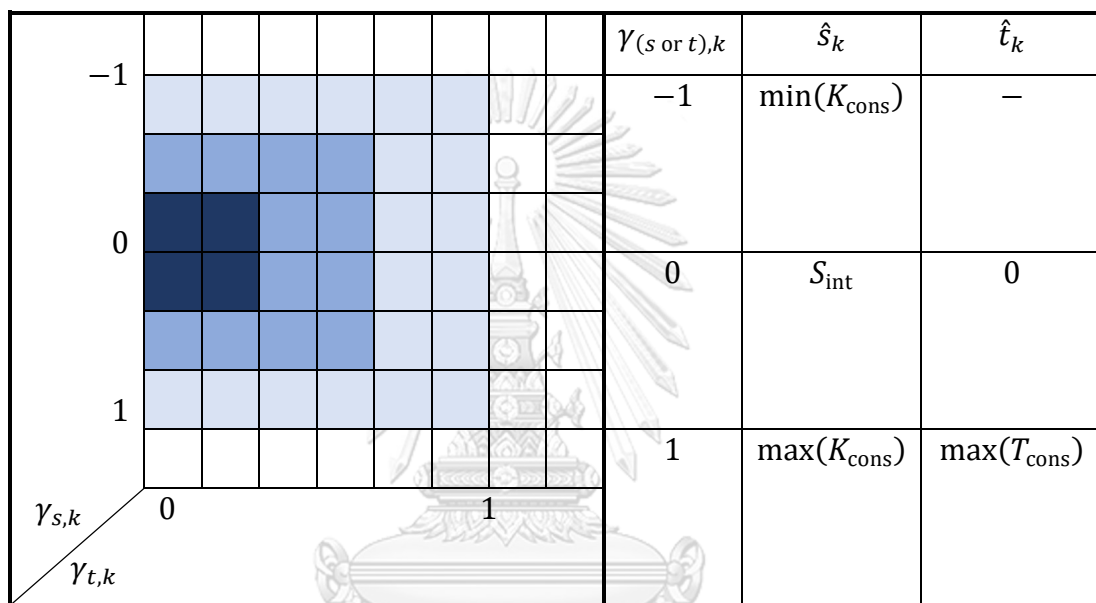
Figure 2: *Possible Area of Effect in Specifying Knots with Interpretation*

3.6. Practical Consideration When Locating the Knots.

Unfortunately, the Matlab spline toolbox [8] cannot return a complete volatility surface from non-meshed knots directly. The function `griddata('cubic')` allows us to use non-meshed input to generate a meshed cubic spline output, but this function cannot extrapolate the values that are not covered by the non-meshed input's boundary. On the contrary, the function `interp2('spline')` can do the extrapolation from meshed inputs only. To be more flexible in using Matlab to generate a bicubic spline surface, we implement a newly-created custom function called `gensplinesurf(*)`. This function applies both `griddata('cubic')` and `interp2('spline')` to initially form an incomplete meshed surface and then extrapolate the remaining values to obtain the

whole volatility surface. We provide Figure 3 to show an idea how the original and the new functions can generate gridded values from some specified knots.
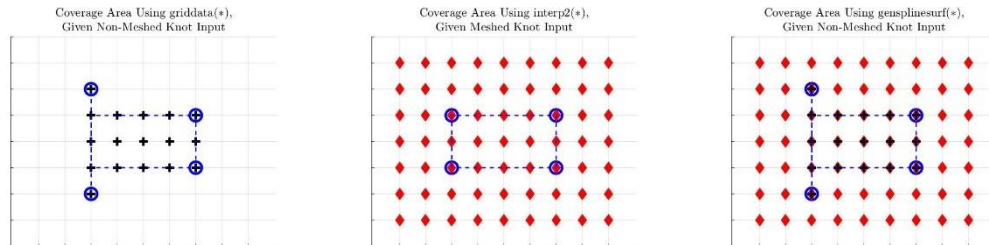
Figure 3: *Coverage Area in Generating a Surface When Using Different Functions*

To explain the meaning of each component in Figure 3 and 4, the blue circles imply the knots' location, and the blue dashed-lines are to draw a possible boundary to create a meshed format. `griddata('cubic')` can only approximate the values at the black '+' markers; meanwhile, `interp2('spline')` can compute the values at the red diamond markers. As a result, we can generate a complete volatility surface by using the knots' specifications that have the blue dashed-lines forming at least one rectangular mesh. Nevertheless, the custom function `gensplinesurf(*)` still has some limitation owing to those two Matlab functions' limited capabilities. Some patterns of knots' placement (see some examples in Figure 4) cannot be used to generate a complete volatility surface.

Figure 4: *Samples of Illegal Patterns of Knot Placement*

Although Matlab functions do not allow us to place the knots in the certain patterns above, we believe that the volatility surface that could have been generated by these illegal patterns should be generatable by the layouts that we are able to implement.

4. Market Data Acquiring.

Since more realistic results are required in studying the characteristics of the implied volatility knots for pricing European options in Thailand, the daily prices of European SET50 call and put options and their MIV from the beginnin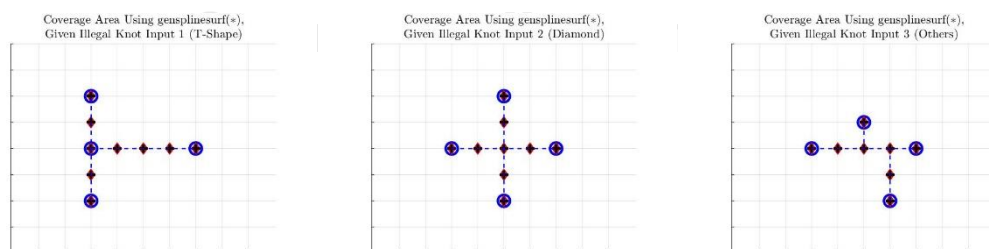g of July to the end of December in 2020 (6 months) are collected and considered as the most recent market data that we are able to acquire from Bloomberg terminal. All the options that we can access, however, have less than 1 year of time to maturity with different strike prices referring to the daily trading data. Furthermore, to approximate option values with the generalized Black-Scholes equation, we need to acquire the other necessary variables, which are initial underlying prices, constant dividend rate, and constant risk-free interest rate from the market information following the dates of downloaded option prices. More specifically, non-dividend SET50 Index prices, S_{int}, are acquired from the time-series data of SET50 Futures via Bloomberg terminal, and it also provides the dividend rate q that we can acquire from the average of SET50's dividend yields. The last considered variable r is acquired from the average of Thai BMA government bond yields.

5. Experimental Results.

In the connection with the end of Sub-section 3.5, the appropriate specification of knots should lead to an accurate option pricing that we do not need to recalibrate the volatility surface frequently. To infer which characteristic of the knots is appropriate in pricing options, the idea to compare root-mean-square error (RMSE) of different specifications in (8) can be a criterion with all the information mentioned in Section 4. In comparing RMSE, we firstly consider that a volatility surface is calibrated daily, so we can observe all the daily prices of call and put options on day $d \in \mathcal{D}$, where $\mathcal{D} = \{1, \ldots, D\}$ is the set of day indices. For example, $d = 1$ represents the first day in our dataset, and $d = D$ represents the last day in our dataset. On day d, we may rearrange (8) and write a new optimization problem,

$$\min_{\hat{\sigma}^{(d)} \in \Sigma} f^d\big(\hat{\sigma}^{(d)}\big) \overset{\text{def}}{=} \frac{1}{N_d} \sqrt{\sum_{n=1}^{N_d} \big\{v_{n,d}\big(\text{BCS}(s,t;\hat{\sigma}^{(d)})\big) - \text{mid}_{n,d}\big\}^2}, \quad d \in \mathcal{D}, \tag{10}$$

subject to $\quad l \le \hat{\sigma} \le u,$

where N_d is the total number of the options on day d and $\text{mid}_{n,d}$ is the mid-price of the option n on day d. The objective function $f^d\big(\hat{\sigma}^{(d)}\big)$ implies the RMSE on day d computed with $\hat{\sigma}^{(d)}$ that is the set of volatility knots calibrated with the option data on day d. Finally, we have D values of RMSE by changing d in (10), and we may define a time-series vector of daily RMSE values that

$$f\big(\hat{\sigma}^{\text{day}}\big) = \big[f^1\big(\hat{\sigma}^{(1)}\big) \quad \dots \quad f^D\big(\hat{\sigma}^{(D)}\big)\big]'$$

where the superscription "day" implies that the volatility surface recalibrates daily. Moreover, the set of volatility knots can be numerous by specifying $\Gamma_{p,\hat{p}}$ from Sub-section 3.5 differently, we can write that

$$f\left(\hat{\sigma}^{\text{day}}_{p,\hat{p}}\right) = \left[f^1\big(\hat{\sigma}^{(1)}_{p,\hat{p}}\big) \quad \dots \quad f^D\big(\hat{\sigma}^{(D)}_{p,\hat{p}}\big)\right]'.$$

We can write a vector describing number of options on any given day $d \in \mathcal{D}$, $N_{\mathcal{D}} = [N_1 \quad \dots \quad N_D]'$. Meanwhile, the condition of p in Sub-section 3.2 that $3 < p \le \min(N_{\mathcal{D}})$ is still held. In practice, the number of p reflects the number of decision variables in (10), so we may select some numbers of $p \in \{4, \dots, p_{\text{max}}\}$ where p_{max} is the maximum number of p that matters in computation. On the contrary, $\hat{p}$ represents the number of the location sets in placing p knots, so $\hat{p}$ can be any positive finite integers. For a notation purpose, let $\hat{p}_{\text{last}}$ be the last specification of p_{max} knots case. Consequently, we can create a matrix of RMSE values,

$$F\big(\hat{\sigma}^{\text{day}}\big) = \left[f\big(\hat{\sigma}^{\text{day}}_{4,1}\big) \quad \dots \quad f\left(\hat{\sigma}^{\text{day}}_{p_{\text{max}},\hat{p}_{\text{last}}}\right)\right],$$

where each row refers to RMSE values on any day indices, and each column implies each specification of knots. In addition, for a comparison purpose, we can compute the rate of RMSE's change over Spec. 1 using Spec. 2 on a given day d,

$$1 - f^d\big(\hat{\sigma}^{(d)}_{\text{Spec. 2}}\big)\big/f^d\big(\hat{\sigma}^{(d)}_{\text{Spec. 1}}\big). \tag{11}$$

In our experiment, we consider 1-Constant Volatility Model as a reference model for comparing with other specifications of knot, so we call the *improvement rate* of Spec. p-$\hat{p}$ in short for the rate of RMSE's change over 1-Constant Volatility Model using Spec. p-$\hat{p}$.

Next, Sub-section 5.1 explains some steps to choose a number of knots that produces acceptably small values of RMSE, and we continue to place the knots at different locations and evaluate their RMSE in Sub-section 5.2. Moreover, since a volatility surface possibly provides some forward-looking volatility values at a given time and stock price. A volatility surface assuming option prices today contains some future information, so we should be able to use that surface to price options in future. However, diverse specifications of knot probably generate different patterns of volatility surface that is able to price future options for some time after calibration at acceptable level of accuracy. This point, thus, is explained in detail in Sub-section 5.3. After gathering all those experiment results, we can show some samples of patterns and make some conclusions in Sub-section 5.4.

5.1. Number of Knots.

To explain the result in specifying the different numbers of knots to price options in detail, we initially consider the least number of knots that can generate a non-flat volatility surface or $p = 4$. We lay those four knots at different sets of location (see in Figure 5) with respect to our hypothesis in Figure 2; however, the detail in locating volatility knots is further explained in Sub-section 5.2.
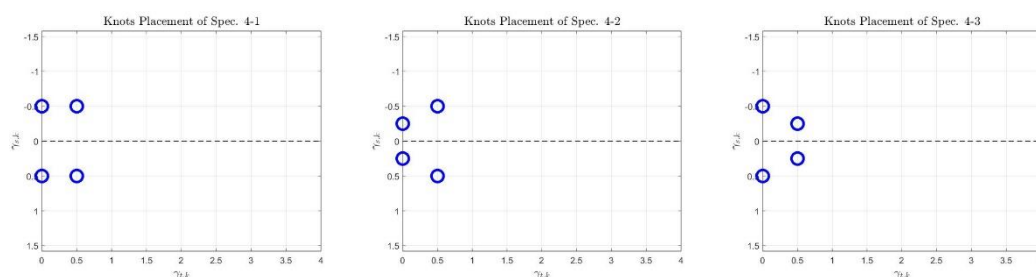

Figure 5: *Samples of 4-Knots' Placement*

After we have some sample patterns of 4-knot, we can calibrate a volatility surface and compute RMSE on each day with respect to those different 4-knot specifications by (10). We, furthermore, obtain the improvement rate of Spec. 4-$\hat{p}$ where $\hat{p} = 1, 2,$ and 3 with the idea in (12). Later, we can plot the percentage of improvement by using different 4-knot specifications in Figure 6.
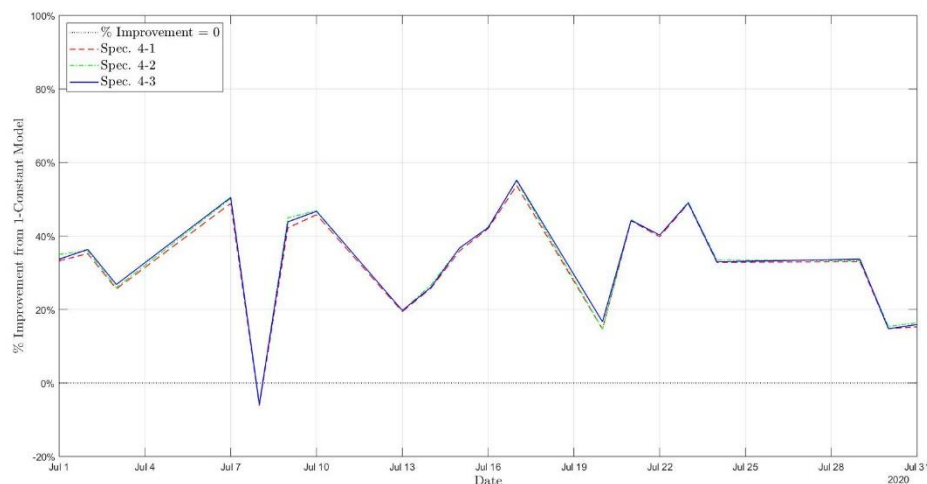

Figure 6: *Daily Percentage Improvement in RMSE*
(Over 1-Constant Volatility Model) Using Different 4-Knot Placements

To explain our hypothesis, a plane on 3-dimensional spaces can be identified by specifying any three coordinates. If we calibrate a volatility surface using only three knots, the surface will be identical for every pattern of knot placement to best fit the market. 4-knot specifications, on the other hand, are only to add one more knot to create a non-flat surface, so the patterns of volatility surfaces generated by four knots are not very diverse in our view. Consequently, Figure 6 barely provides us an observable difference. Later, we consider different 5-knot specifications to generate a volatility surface and compute the RMSE value and the improvement rate of 1-Constant Volatility Model. However, with the further tests, we can conclude that the most appropriate number of knots is five, so the patterns of 5-knot placement are shown in Sub-section 5.2 to study for the most suitable location. To continue our process in finding the most appropriate number of knots, we compare the improvement rate of 1-Constant Volatility Model by using 4-knot and 5-knot

specifications. By the same method in acquiring Figure 6, we can plot Figure 7. We can observe that the improvement rate of the 5-knot candidate is never lower than the 4-knot's, so this implies that using 5 knots is better than using 4 knots in generating a volatility surface for pricing options.
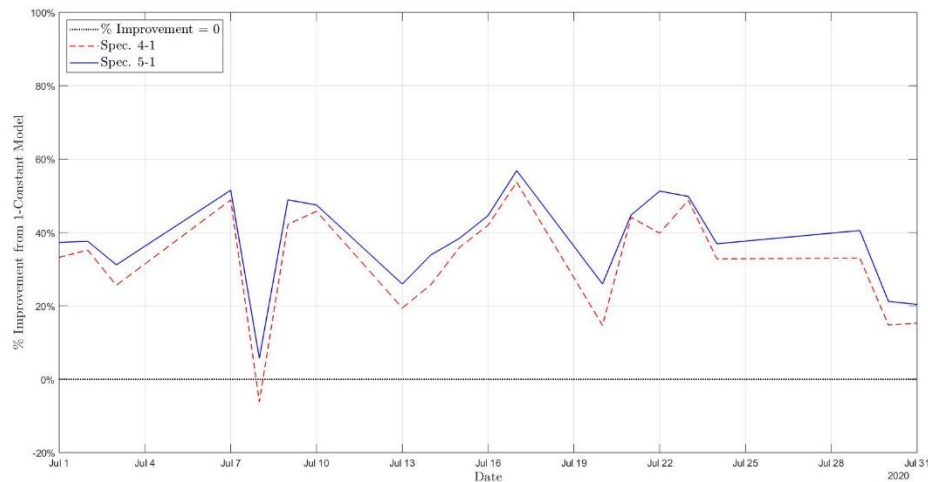
Figure 7: *Daily Percentage Improvement in RMSE*
(Over 1-Constant Volatility Model) Using Spec. 4-1 and Spec. 5-1

Our next study is to use 6 knots to generate a volatility surface, so we consider some 6-knot specifications in Figure 8. After that, we can compute both the RMSE value and the improvement rate. We would like to compare 6-knot and 5-knot specifications; hence, we plot their improvement rate of 1-Constant Volatility Model in Figure 9.
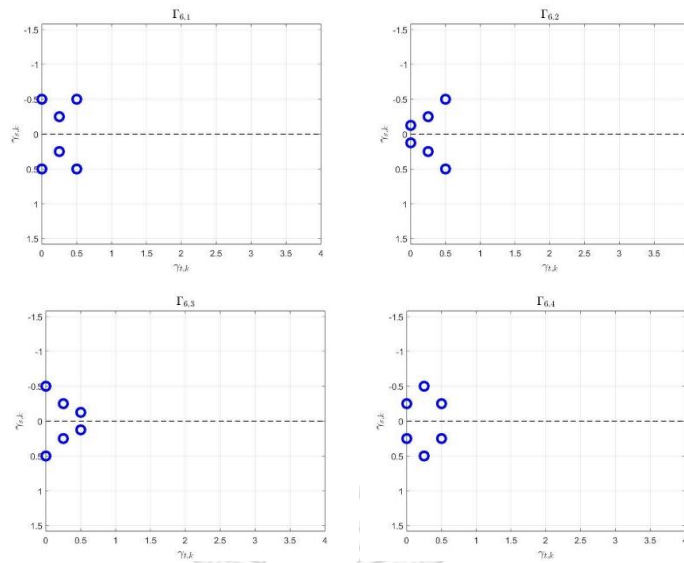
Figure 8: *Samples of 6-Knots' Placement*
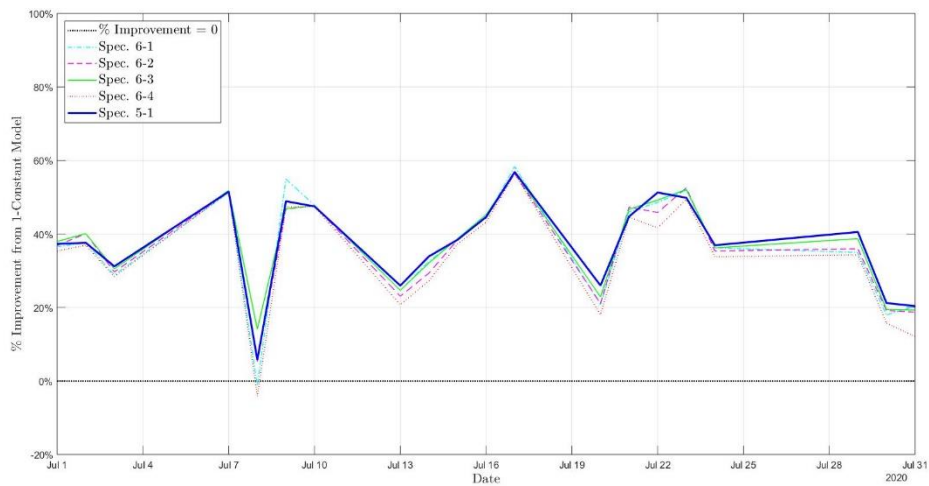
Figure 9: *Daily Percentage Improvement in RMSE*
(Over 1-Constant Volatility Model)
Using Different 6-Knot Specifications and Spec. 5-1

To interpret the results in Figure 9, using 6 knots to generate a volatility surface cannot distinctively outperform the 5-knot specification that has smaller number of decision variables in term of the improvement. This means that we spend longer time in computation 6-knot variables but obtain no better result than the 5-knot specification. Nevertheless, to prove our hypothesis more concretely, we compare the best 4-knot and 6-knot specifications (Spec. 4-1 and Spec. 6-3) with the 5-knot

candidate. In other words, for all day $d \in \mathcal{D}$, we can compute the improvement rate of RMSE's change with respect to increment of knot's number by

$$1 - f^d\left(\hat{\sigma}_{5,1}^{(d)}\right)/f^d\left(\hat{\sigma}_{4,1}^{(d)}\right) \quad \text{and} \quad 1 - f^d\left(\hat{\sigma}_{6,3}^{(d)}\right)/f^d\left(\hat{\sigma}_{5,1}^{(d)}\right).$$

Moreover, we can also compare the computational time increment when adding more knots by implementing Matlab's function `tic-toc` while using 4, 5, or 6 knots to calibrate a set of volatility knots. As a result, the median of the computational time using different number of knots $p =4$, 5, and 6 is 7.4, 13.1 and 27.6 seconds, respectively. We can report both the percentage improvement and computational time increment when changing number of knots by Table 1.

	Number of Knots Changed From	
	4 to 5	5 to 6
Median of % Improvement in RMSE	6.44%	0.81%
Median of Computational Time Increment (sec)	5.7	14.5
	$(13.1 - 7.4)$	$(27.6 - 13.1)$
(%)	77.09%	110.45%

Table 1: *Summary of Statistical Results When Changing Number of Knots*

To interpret the table above, using 5 knots to generate a volatility surface can improve the RMSE values by taking some acceptable computational time at around 13.1 seconds for one calibrating time. Comparing to the 6-knot specification, on the other hand, it can only improve the error term less than 1% but double the time in computation of 5-knot specification. Therefore, the appropriate number of the volatility knots in this research is five.

5.2. Location of Knots.

Right after we conclude the results in Sub-section 5.1, we place five knots with different $\Gamma_{5,\hat{p}}$ for some possible numbers of $\hat{p} = 1,2, ...$ Eventually, we have two best candidates, called Spec. 5-1 and Spec. 5-2, that are shown in Figure 5. To be honest, although Spec. 5-1 and Spec. 5-2 are the sets of knots' specification that best

fit the market prices from all the cases we have tested so far, the daily RMSE results of other patterns of 5-knot specification are not very different. However, some patterns, such as Spec. 5-3 in Figure 10, obviously have higher RMSE on some days, especially in July. To be consistent in comparing RMSE results, the improvement rates using different 5-knot specifications are plotted in Figure 11. This means that the knots' location has an important role in pricing options of SET50 Index.
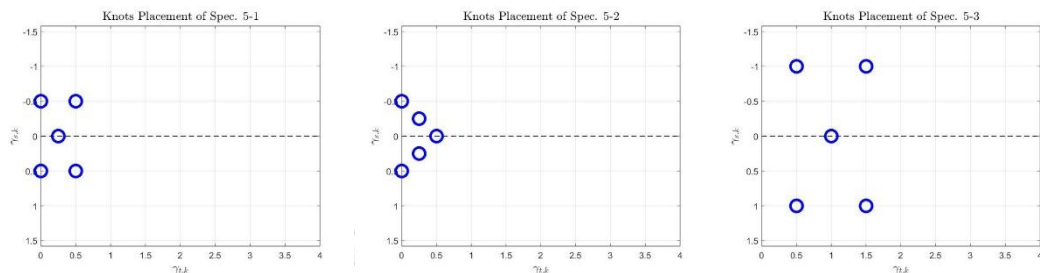

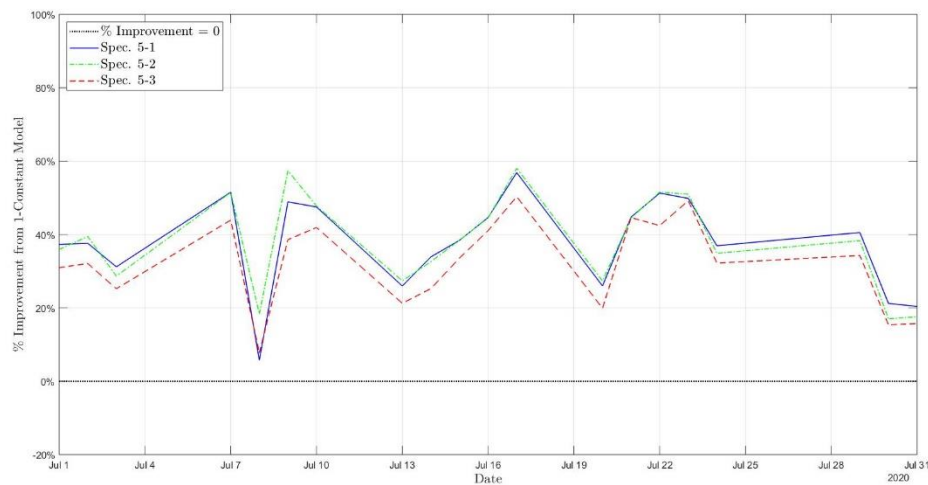Figure 10: *Samples of 5-Knot Placements*

Figure 11: *Daily Percentage Improvement in RMSE (Over 1-Constant Volatility Model) Using Different 5-Knot Specifications in July*

To summarize the characteristics of 5-knot placement that are acceptably accurate in SET50 Index's option pricing with all the collected results, we may choose the knots' location with two main ideas.

- All the knots laid symmetrically with respect to $\gamma_{s,k} = 0$ (or $s = S_{\text{int}}$) can generate better results, and one knot should be on that line.
- Placing knots at $(\gamma_{t,k}, \gamma_{s,k})$ close to $(0,0)$ or (s,t) close to $(S_{\text{int}}, 0)$ generate less RMSE than placing them further away, and two knots should be located at $\gamma_{t,k} = 0$ or $t = 0$.

Nonetheless, although we have tried as many as possible specifications of knot and obtain two best candidates as shown in Figure 10, the daily RMSE value on some days is still high and cannot be reduced to our target, 20% improvement of RMSE computed by the 1-Constant Volatility Model (see in Figure 12).
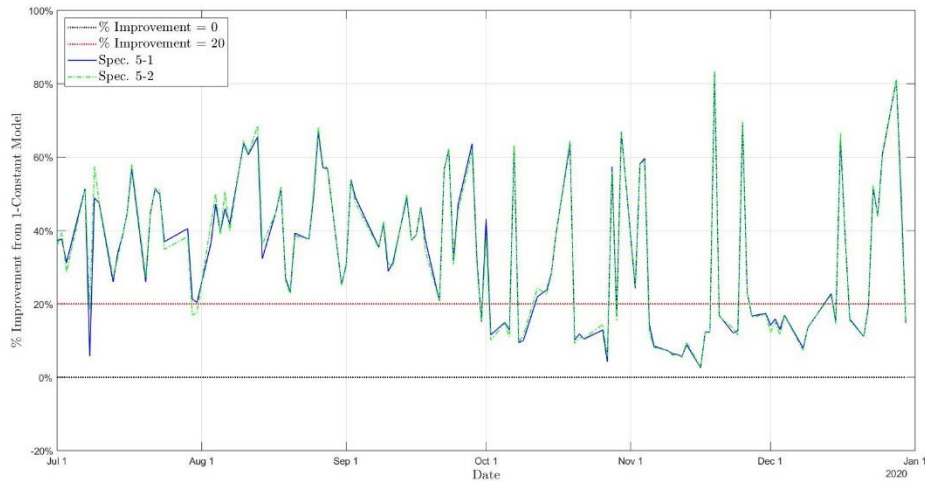
Figure 12: *Daily Percentage Improvement in RMSE*
(Over 1-Constant Volatility Model) Using Spec. 5-1 and Spec. 5-2 with 20% Target

However, we detect two characteristics of the market strike and MIV relationship that causes inaccurate option pricing (see some examples in Figure 13), and we can describe the two abnormal characteristics with these following statements.

- The $K = S_{\text{int}}$ line crosses the K-MIV curve at any point on a high-frown shape.
- The K-MIV curve gradually skews from $K = K_{\text{min}}$ on a given day until MIV values sharply increase at K values around the second or third largest strike on that day.
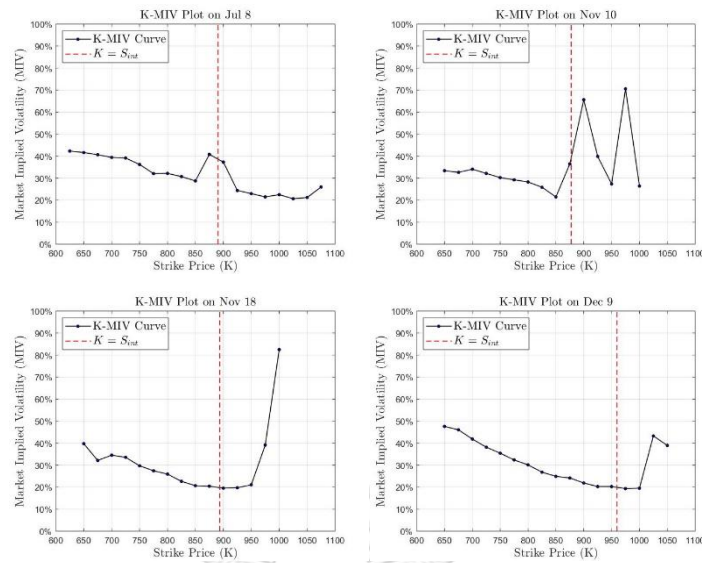
Figure 13: *The Characteristics of K-MIV Plot Causing Inaccurate Option Pricing*

We may consider these two characteristics of K-MIV plot that affects pricing accuracy of a calibrated volatility surface as an abnormal market situation that leads to a mispricing problem. Unfortunately, we still cannot find any specification that fits those characteristics better than both Spec. 5-1 and Spec. 5-2.

5.3. Recalibrating Period of Knots.

After we have some specifications of knot from the results in Sub-section 5.2, we continue to test how long each specification can be used by considering three recalibrating types that are daily, weekly, and monthly. For the daily recalibration, the results are obtained from Sub-section 5.2, but the other two types are to reduce the frequency of recalibrating process. The longer recalibrating period means that once we calibrate a volatility surface on a given day d_0, we then use that surface for L_d working days long including day d_0 where L_d is a non-negative integer. In other words, we may describe by adjusting the objective function in (10) that is

$$
f^d(\hat{\sigma}^{(d_0)}) = \frac{1}{N_d}\sqrt{\sum_{n=1}^{N_d}\{v_{n,d}(\mathrm{BCS}(s,t;\hat{\sigma}^{(d_0)})) - \mathrm{mid}_{n,d}\}^2},
\tag{12}
$$

$$
d_0 \in \mathcal{D}, \ \text{and} \ d \in \{d_0, d_0 + 1, \dots, d_0 + (L_d - 1)\}.
$$

In this paper, we consider L_d at 5 for weekly and 20 for monthly recalibrating periods. Moreover, since we would like to compare the daily recalibrating results in (11) with other periods in recalibration, we start the first calibration of the volatility surface on day 1 and consider that

$$f\left(\hat{\sigma}_{p,\hat{p}}^{\text{period}}\right) = \left[f^1\left(\hat{\sigma}_{p,\hat{p}}^{(1)}\right) \quad \dots \quad f^{L_d}\left(\hat{\sigma}_{p,\hat{p}}^{(1)}\right) \quad f^{L_d+1}\left(\hat{\sigma}_{p,\hat{p}}^{(L_d+1)}\right) \quad \dots \quad f^D\left(\hat{\sigma}_{p,\hat{p}}^{(\rho L_d+1)}\right)\right]',$$
$$\exists \rho = 0, 1, \dots, \lfloor D/L_d \rfloor - 1,$$

where $\rho + 1$ implies the number of times in recalibration to cover all the time-series data. For example, $\rho + 1 = 20$ for 120 days of option data implies that the volatility surfaces are recalibrated 20 times along 120 days at the equal period of time, which is $L_d = 5$. The superscription "period" refers to different periods in recalibration; in this case, we may substitute "period" with "week" for $L_d = 5$ and with "month" for $L_d = 20$. With the similar idea in (11), we can also form two matrices of RMSE values that use volatility surfaces recalibrated weekly and monthly,

$$F\left(\hat{\sigma}^{\text{week}}\right) = \left[f\left(\hat{\sigma}_{4,1}^{\text{week}}\right) \quad \dots \quad f\left(\hat{\sigma}_{p_{\max},\hat{p}_{\text{last}}}^{\text{week}}\right)\right], \quad \text{and}$$
$$F\left(\hat{\sigma}^{\text{month}}\right) = \left[f\left(\hat{\sigma}_{4,1}^{\text{month}}\right) \quad \dots \quad f\left(\hat{\sigma}_{p_{\max},\hat{p}_{\text{last}}}^{\text{month}}\right)\right].$$

With the candidates' specification mentioned in Sub-section 5.2, we plot Figure 14 to see the daily RMSE's improvement rate using Spec. 5-1's and Spec. 5-2's with different periods in recalibration.
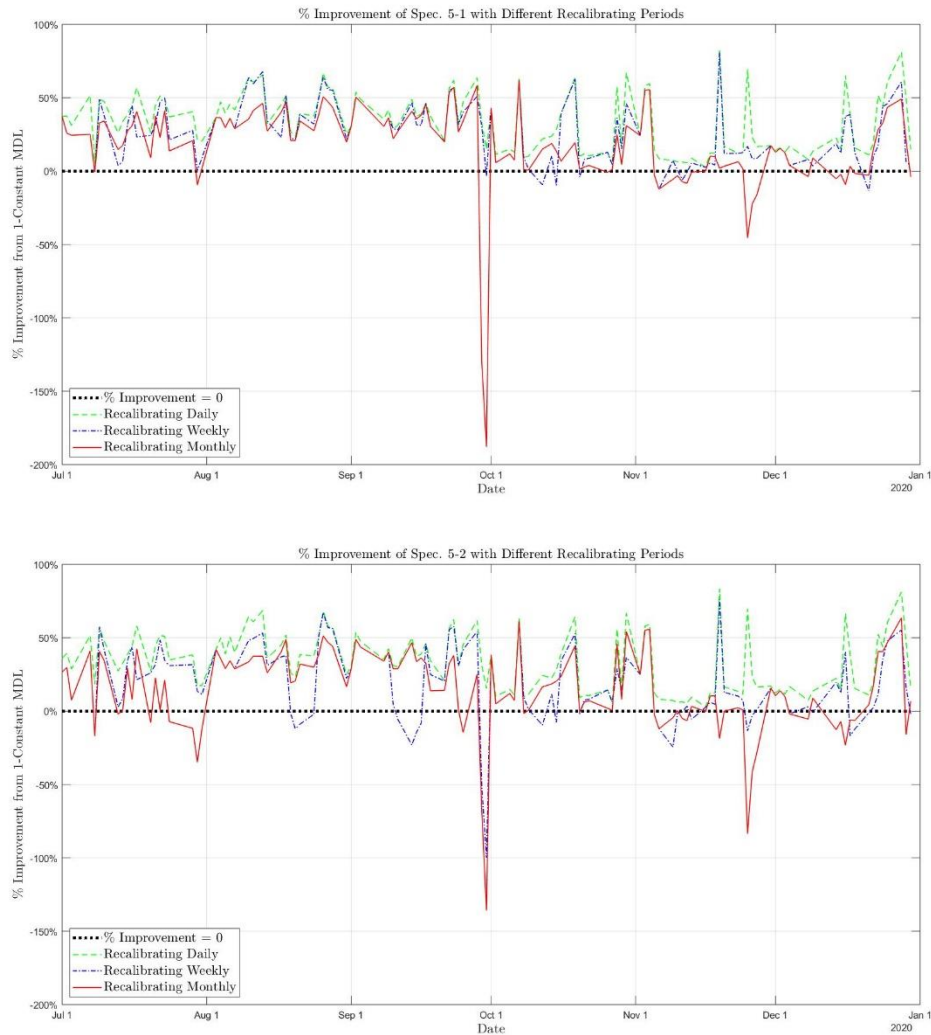
Figure 14: *Daily Percentage Improvement in RMSE*
(Over 1-Constant Volatility Model) Using Spec. 5-1 and Spec. 5-2
with Different Periods in Recalibration

To interpret the results in Figure 14, when we use a volatility surface to price options that are not in the calibration dataset, the longer time that we use the same surface without recalibration tends to increase the error term, especially in the monthly results of both specifications. Furthermore, to distinguish which specification is better, we also provide some scatter plots in Figure 15 to see the relationship of the daily RMSE values generated by Spec. 5-1 and Spec. 5-2 on the same days with daily, weekly, and monthly recalibration periods of the volatility surfaces.
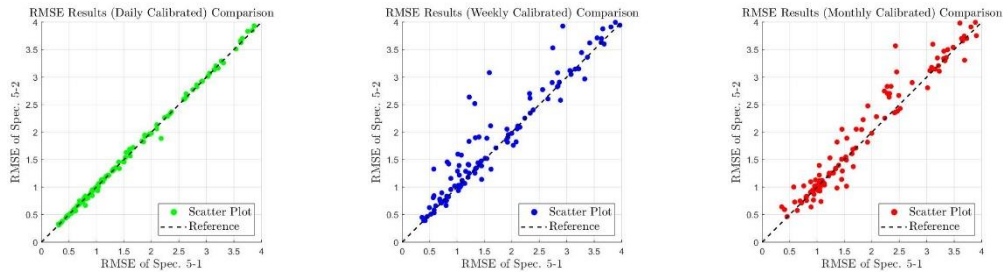
Figure 15: *Scatter Plots of Daily RMSE Values Generated by Spec. 5-1 and Spec. 5-2 with Different Periods in Recalibration*

Explaining the results in Figure 15, when the points are so close to the vertical axis, Spec. 5-1 can be considered good in pricing. We can also consider Spec. 5-2 with the same idea but close to the horizontal axis instead. Considering at the coordinate $(0,0)$ of the three plots in Figure 10, the longer period before recalibration makes the scatter plots further away from $(0,0)$, and this implies that using a volatility surface longer without recalibration causes greater values in daily RMSE. In addition, the reference line is only to represent the line that RMSE of Spec. 5-1 equals RMSE of Spec. 5-2, so the distance from the line to scatter points can interpret which specification performs better in pricing options. Even though the daily calibrated results do not identify any advantage of both the candidates, Spec. 5-1's weekly calibrated results seem clearly better than Spec. 5-2's. Speaking of the monthly calibrated result, since its plot scatters away from not only the coordinate $(0,0)$ but also the reference line without any trend, we should not rely on the monthly calibrated volatility surfaces in pricing options. Otherwise, we might encounter a mispricing problem as mentioned earlier. To support our observation, we also count the days that our considered specifications of knot recalibrated weekly and monthly perform worse than 1-Constant Volatility Model to report in proportional format in Table 2.

	Recalibrating Period	
	Weekly	Monthly
Spec. 5-1	8.33%	18.33%
Spec. 5-2	23.33%	25.83%

Table 2: *Proportion of Days Where Each Specification Perform Worse Than 1-Constant Volatility Model's RMSE*

From the result in Table 2, we do not recommend recalibrating the volatility knots monthly with either specification. Otherwise, the error term generated by any calibrated set of volatility knots is possibly larger than using the 1-Constant Volatility Model that does not match the market in practice. To conclude all the results in this sub-section, we prefer Spec. 5-1 to Spec. 5-2 for generating a volatility surface, and the surface should be recalibrated within five working days after its first estimation.

5.4. Patterns of Calibrated Volatility Surfaces.

After completing all the previous experiments, we expect to see some common patterns of calibrated volatility surfaces. Therefore, some samples of the calibrated volatility surfaces with the candidate specifications in Sub-section 5.2 can be illustrated in this sub-section. However, since there are various patterns of generated volatility surfaces, we set some conditions to classify those surfaces in four patterns displayed in Figure 17.
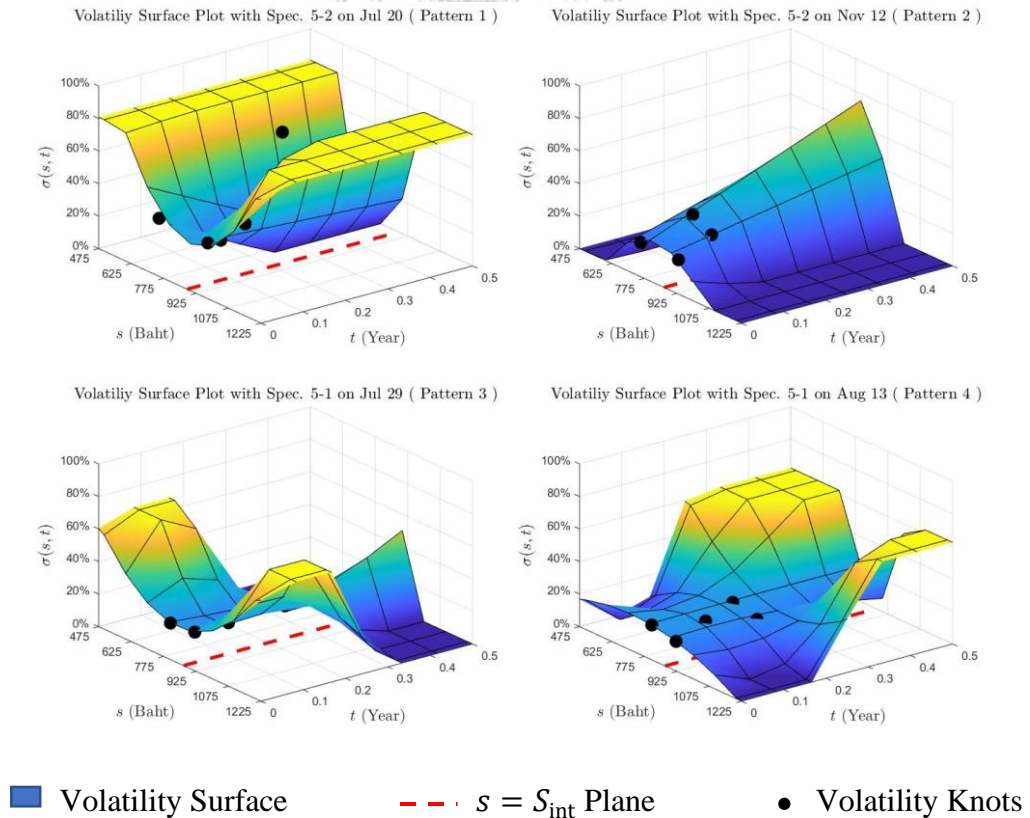

Figure 16: *Sample Patterns of Calibrated Volatility Surfaces*

Speaking of the pattern classification, we start to observe the cross-section of a volatility surface perpendicular to t-axis at three values of $t_j = \tau_c$ for $c = 1, 2, 3$ where

$$\tau = [\tau_1 \quad \tau_2 \quad \tau_3] = [0 \quad 0.5 \max(T_{\text{cal}}) \quad \max(T_{\text{cal}})].$$

We can consider that the number of c implies the cth cross-section. At this point, we have three curves of $(s_i, \sigma_{i,j})$ with respect to the considered t_j. Next, we can locate s_i where $\sigma_{i,j}$ are the local extrema of each curve. Moreover, the coordinates of $(s_i, \sigma_{i,j})$ where $i = 1$ and N_s are to observe the volatility values at the edges of s-axis. For simplicity, we may define some vectors and matrices, for $c = 1, 2, 3$,

$$C_c = [\bar{s}_c \quad \bar{t}_c \quad \bar{\sigma}_c],$$
$$\bar{s}_c = [s_1 \quad s_{(c,1)} \quad \cdots \quad s_{(c,\bar{c})} \quad s_{N_s}]'$$
$$\bar{t}_c = \tau_c \cdot \mathbf{1}_{\text{size}(\bar{s}_c)}, \qquad \text{and}$$
$$\bar{\sigma}_c = \sigma(\bar{s}_c, \bar{t}_c).$$

To explain all the notations, c is the number to specify the curve number of the three cross-sections mentioned earlier, and C_c implies all the coordinates $(s_i, t_j, \sigma_{i,j})$ to draw the cth curve. The vector $\bar{s}_c$ consists of s values laid on the cth cross-section. However, the local extrema on a curve can be any number, so we consider that the cth curve has $\bar{c}$ local extrema. The variable $s_{(c,\bar{c})}$ implies s value at the $\bar{c}^{\text{th}}$ extremum of the cth curve, and $s_1 \le s_{(c,1)} \le \cdots \le s_{(c,\bar{c})} \le s_{N_s}$. To be consistent for the size of curves' coordinates, $\bar{t}_c$ is only a vector form of τ_c at any considered cross-sections, and $\mathbf{1}_{\text{size}(\bar{s}_c)}$ is an all-ones vector at the same size of $\bar{s}_c$. Finally, we have $\bar{\sigma}_c$ that is the vector of the volatility values on the cth curve.

By applying the idea with the real data of 5-knot specifications, the curve at different time $t_j = \tau_c$ has only one the local extremum $\sigma_{i,j}$ with respect to s_i. Thus, the elements' number of vector $\bar{s}_c$ can be reduced to three, so can $\bar{t}_c$ and $\bar{\sigma}_c$. For any $c = 1, 2, 3$, the size of C_c is also reduced to 3×3. This means that each of the cth curve now has only three coordinates $(s_1, \sigma_{1,j})$, $(s_{\text{LE}}, \sigma_{\text{LE},j})$, and $(s_{N_s}, \sigma_{N_s,j})$ where the subscription LE implies the values of s and σ at the local extremum and $s_1 \le s_{\text{LE}} \le s_{N_s}$.

After that, we can classify the curves by two shapes which are *Smile* and *Frown*. When a curve has the result of $\min(\sigma_{1,j}, \sigma_{\text{LE},j}, \sigma_{N_s,j}) = \sigma_{\text{LE},j}$, it has Smile shape. In contrast, the Frown shape occurs when a curve has $\max(\sigma_{1,j}, \sigma_{\text{LE},j}, \sigma_{N_s,j}) = \sigma_{\text{LE},j}$. Next, since we have three curves in consideration, we can order their shape using the number of c. Finally, we are able to classify all four patterns in Figure 16 by the conditions shown in Table 3.

	The Shape of Curve at c Equals		
Pattern's Name	1	2	3
Always-Smile	Smile	Smile	Smile
Always-Frown	Frown	Frown	Frown
Smile-Then-Frown	Smile	Smile or Frown	Frown
Frown-Then-Smile	Frown	Frown or Smile	Smile

Table 3: Conditions in Classifying Pattern of Volatility Surfaces

To observe the patterns of volatility surfaces generated by the 5-knot candidates more precisely, we can report the occurrence rate of each pattern in Table 4 by considering the proportion of days that Spec. 5-1 and Spec. 5-2 can generate different patterns of volatility surfaces.

		Occurrence Rate	
	Description	Spec. 5-1	Spec. 5-2
Pattern 1	Always-Smile	24.17%	73.33%
Pattern 2	Always-Frown	16.67%	12.50%
Pattern 3	Smile-Then-Frown	30.83%	2.50%
Pattern 4	Frown-Then-Smile	27.50%	3.33%
Others	–	0.83%	8.33%

Table 4: *Occurrence Rate of Volatility Surfaces' Patterns*

To interpret the result in Table 4, Spec. 5-1 seems more flexible to generate a volatility surface because all the four patterns are most likely to occur at average. On the contrary, Spec. 5-2 mostly generate Always-Smile patterns of volatility surfaces.

In summary, we can describe the possible patterns of volatility surfaces in pricing options by these three characteristics.

- Both Spec. 5-1 and Spec. 5-2 require first 4 knots that possibly create meshed grids as a non-flat reference surface. Meanwhile, the last knot on $s = S_{\text{int}}$ plane is most likely to form the main curvature of the smile or a little frown shapes.

- Spec. 5-1, compared to Spec. 5-2, is more able to produce varying degree of curvature along the time to expiration. To state the possible reason, Spec. 5-1 has two knots at the position which is the furthest from $t = 0$, but Spec. 5-2 has only one knot at that position. Two knots may create more nonlinearity for the surface than one knot. For these reasons, Spec. 5-1 possibly performs better than Spec. 5-2 as a result in Sub-section 5.3.

- The $s = S_{\text{int}}$ plane tends to separate the smile shape of the volatility surfaces' cross-section into two symmetric parts. Furthermore, when that plane crosses smile shapes at any time t, the volatility values at the intersection seem to be the vertex of those smiles.

6. Conclusion.

To price options of an underlying, it is assumed to follow a continuous 1-factor diffusion model. Its volatility function $\sigma(s, t)$, also considered as the volatility surface, is approximated by using a bicubic spline technique, one of smoothness approaches, to generate some representative knots to express the whole surface at all possible coordinates of stock price s and time to expiration t. We firstly fix the initial values of volatility knots and use them to price call and put options with available strikes and maturities in the market. Later, we solve an optimization problem that has those volatility knots as decision variables to minimize the objective function of root-mean-square error, RMSE, in between the model and market option prices. Meanwhile, the knots can be specified differently by considering their number and locations on the possible measurable space of s and t.

With the data of SET50 Index and its options in Section 4, we can observe the effect on pricing accuracy by using different specifications of knot to solve (10). Candidates of knots' specification can generate the volatility surface that fit the model option prices with the market appropriately. We found that specifying 5 knots of volatility values is sufficiently accurate in pricing SET50 Index options. For the effective location of those 5 knots on s-t plane, they should be placed close to $s = S_{\text{int}}$ and $t = 0$ as shown in Figure 2, and we have two candidates of specification called Spec. 5-1 and Spec. 5-2 in consideration. Later, we do another experiment to observe how long a volatility surface can be used before recalibration. We compute the daily RMSE values of the candidates' specification in the previous experiment but consider in recalibrating the volatility surfaces daily, weekly, and monthly. Spec. 5-1, as a result, can price options within five working days after its first calibration. In contrast, Spec. 5-2 produces unacceptable daily RMSE values when using its volatility surfaces on a few days after the calibration date. All the prior experiments imply that specifying the volatility knots at the right number and locations are necessary to price options sufficiently accurately. Nevertheless, some market factors, such as the MIV plot with respect to strike prices, may affect the accuracy in pricing options even though the knots' specification can price options precisely on most days in the dataset.

Finally, we illustrate four common patterns of the 5-knot volatility surface of which specifications perform well in the prior experiments. Four of the five knots are to create meshed grids as a non-flat reference surface while the other one is to form the main curvature of the volatility surface. We typically see the pattern of smile or a little frown along s-axis for all t on the generated volatility surfaces, and the $s = S_{\text{int}}$ plane tends to separate the smile or a little frown shape symmetrically. Moreover, the volatility values on that plane seem to be the vertices of smiles. The more nonlinear property of the volatility surface's cross-section taken perpendicular to t-axis possibly causes the better results when using the volatility surface longer than its calibration date. The importance, methods, and results in specifying volatility knots to price European options are identified.

REFERENCES

1. Andersen, L. and R. Brotherton-Ratcliffe, *The equity option volatility smile: an implicit finite-difference approach.* Journal of Computational Finance, 1998. **1**(2): p. 5-37.
2. Avellaneda, M., et al., *Calibrating volatility surfaces via relative-entropy minimization.* Applied Mathematical Finance, 1997. **4**(1): p. 37-64.
3. Birkhoff, G. and C.R. De Boor, *Piecewise polynomial interpolation and approximation.* Approximation of functions, 1965: p. 164-190.
4. Black, F. and M. Scholes, *The pricing of options and corporate liabilities.* Journal of political economy, 1973. **81**(3): p. 637-654.
5. Bouchouev, I. and V. Isakov, *The inverse problem of option pricing.* Inverse Problems, 1997. **13**(5): p. L11.
6. Cont, R. and J. Da Fonseca, *Dynamics of implied volatility surfaces.* Quantitative finance, 2002. **2**(1): p. 45-60.
7. Das, S.R. and R.K. Sundaram, *Of smiles and smirks: A term structure perspective.* Journal of financial and quantitative analysis, 1999: p. 211-239.
8. De Boor, C., *Spline toolbox for use with MATLAB: user's guide, version 3*. 2005: MathWorks.
9. Derman, E. and I. Kani, *Riding on a smile.* Risk, 1994. **7**(2): p. 32-39.
10. Derman, E., I. Kani, and J.Z. Zou, *The local volatility surface: Unlocking the information in index option prices.* Financial analysts journal, 1996. **52**(4): p. 25-36.
11. Dierckx, P., *Curve and surface fitting with splines*. 1995: Oxford University Press.
12. Dupire, B., *Pricing with a smile.* Risk, 1994. **7**(1): p. 18-20.
13. Hathaway, N., *The non-stationarity of share price volatility.* Accounting & Finance, 1986. **26**(2): p. 35-54.
14. Hull, J. and A. White, *The pricing of options on assets with stochastic volatilities.* The journal of finance, 1987. **42**(2): p. 281-300.
15. Jackwerth, J.C. and M. Rubinstein, *Recovering probability distributions from option prices.* The Journal of Finance, 1996. **51**(5): p. 1611-1631.
16. Lagrado, R. and S. Osher, *Reconciling differences.* RISK-LONDON-RISK MAGAZINE LIMITED-, 1997. **10**: p. 79-83.
17. Lamberton, D. and B. Lapeyre, *Introduction to stochastic calculus applied to finance*. 2007: CRC press.
18. Merton, R.C., *Option pricing when underlying stock returns are discontinuous.* Journal of financial economics, 1976. **3**(1-2): p. 125-144.
19. Merton, R.C., *Theory of rational option pricing.* The Bell Journal of economics and management science, 1973: p. 141-183.
20. Rubinstein, M., *Implied binomial trees.* The journal of finance, 1994. **49**(3): p. 771-818.
21. Shimko, D., *Bounds of probability.* Risk, 1993. **6**(4): p. 33-37.
22. Tikhonov, A.N. and V.Y. Arsenin, *Solutions of ill-posed problems.* New York, 1977: p. 1-30.
23. Vapnik, V., *Estimation of dependences based on empirical data*. 2006: Springer Science & Business Media.

24.   Wahba, G., *Spline models for observational data*. 1990: SIAM.

VITA

NAME   Wisuth Raweerojthanatt

DATE OF BIRTH   27 October 1990

PLACE OF BIRTH Thailand

INSTITUTIONS   King Mongkut's University of Technology Thonburi:
ATTENDED   KMUTT
HOME ADDRESS   84/13 Chareonkrung 80, Bangkorleam,
                         Bangkorleam, Bangkok, 10120